

Astrophysical constraints on the cold equation of state of the strongly interacting matter

Gyuri Wolf

Wigner Research Centre for Physics, Institute for Particle and Nuclear Physics, Theoretical Physics Department

Budapest, 19.06.2026

Collaborators: G. Kasza, J. Takátsy, P. Kovács, J. Bielich-Schaffner

Phys. Rev. D105 (2022) 103014, D108 (2023) 043002.

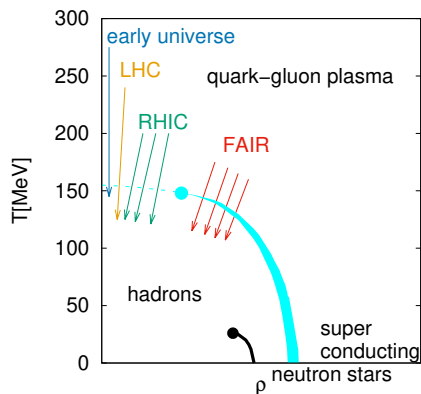
Eur. Phys. J. Spec. Top. (2026), Journal of Subatomic Particles and Cosmology 5 (2026) 100400



Overview

1. Introduction
 - Motivation
 - Structure of neutron stars
 - Observables for dense strongly interacting matter
2. The Quark-meson model
 - The extended Linear Sigma Model
 - Axial(vector) meson extended linear σ -model
 - Parametrization at $T = 0$
 - Results for eLSM
3. EOS
4. Neutron stars
 - Data and constraints
5. Results for Neutron Stars
 - Bayesian inference
 - Results
6. Summary

Dense strongly interacting matter



What is the phase diagram and EOS for dense strongly interacting matter?

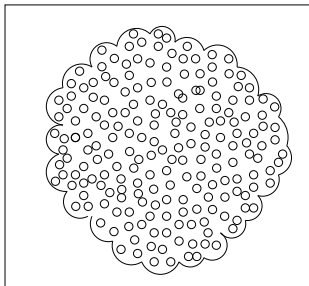
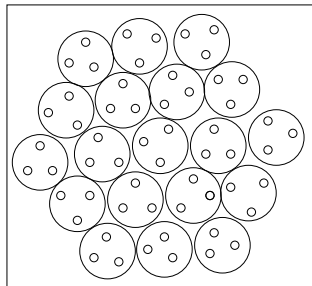
At $\mu = 0$: lattice and experiments (STAR/PHENIX and ALICE).

For $\mu \gg 0$ no precise theory and no heavy ion experiment.

Dense matter at $T=0$

Are there different phases at $T=0$? If yes, at which densities?

heavy ion collisions: no sharp transition until 2-3 ρ_0



$V_{proton} = 2.22 fm^3$ (with r_{em}), densest packing with spheres: 74%
 $\rightarrow \rho_{max} = 0.33 fm^{-3} \approx 1.8\rho_0$ by maximal packing

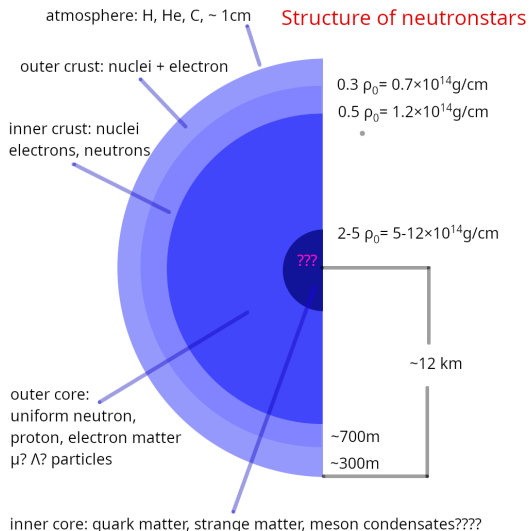
Model: nucleon = core + meson cloud

Reid hard core potential: $r_{hc} \approx 0.5r_{em} \rightarrow \rho_{max} \approx 15\rho_0$ at hard core overlap

Form factors (scalar and vector em, axial vector and gluonic: μ absorption):

$r_{core} = \sqrt{\langle r^2 \rangle} \approx 0.5 fm \rightarrow \rho_{max} \approx 8\rho_0$ at core overlap

Neutron Stars a challenge and a possibility

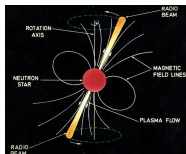


Neutron stars are contain cold, dense matter ($T \approx 0$, $\rho > 3\rho_0$) not available in terrestrial experiments (Laboratory for strong interaction)

What is the structure of neutron stars (what are the constituents), hybrid stars? Superfluids?

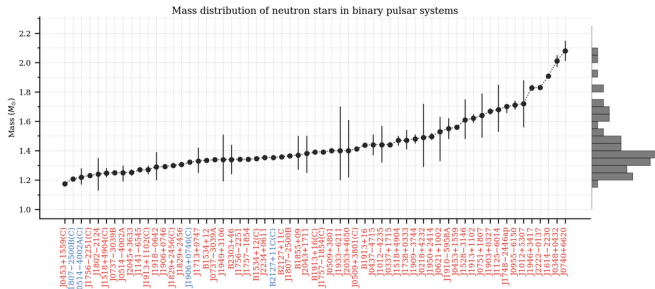
YN, YNN interactions are important, three-body repulsion for Λ , Σ (Weise)

Pulsar mass distribution



lighthouse effect, very precise frequency (1-700 Herz)

Pulsar mass measurements and tests of general relativity



Measurables of Neutron Stars

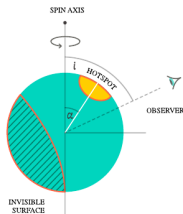
- ▶ mass: in binary systems the orbital motion, Shapiro-decay, $1M_{\odot} \geq M \geq 2.4M_{\odot}$ though limits are not very well known
- ▶ radius: from temperature and radiation, and NICER X measurement 10-15km
- ▶ rotation frequency: 0.1 - 700 H (Kepler-frequency $> 1.4\text{kHz}$)
- ▶ surface temperature $10^{11}\text{K} \sim 10\text{MeV} \rightarrow 10^6\text{K}$, by neutrino radiation (URCA process)
- ▶ magnetic field: $10^8 - 10^{12}$ G, in magnetars $10^{15} - 10^{18}$ G
- ▶ glitches: sudden increase of the frequency (star quakes, vortices in superfluid matter)
- ▶ tidal deformability $\Lambda < 800$

Neutron Star observations

- ▶ Discovering heavy neutron stars $M > 2M_{\odot}$ Demorest, et al., Nature. 467, 1081-1083 (2010). largest mass observed: $2.35 \pm 0.17 M_{\odot}$ (2022) Black Widow (Shapiro-delay: pulsar+another star, at almost full covering the second member of the binary delays the radiation of the pulsar)
- ▶ Advanced gravitation wave detectors: Advanced Ligo, Virgo, Kagra: single neutron stars??. multichannel astronomy
neutron star collision: GW170817 (130 million lightyears)

Modern telescopes: NICER X-ray telescope: precise ($<5\%$) mass and radius measurements (2020) “for nearby” neutron stars,

- ▶ 5 stars yet, but more to come
radiation bent by strong gravity: hotspots observation: M, R



Tolman-Oppenheimer-Volkoff (TOV) equation

Solving the Einstein's equation for spherically symmetric case and homogeneous matter \rightarrow TOV eqs.:

$$\frac{dp}{dr} = - \frac{[\rho(r) + \varepsilon(r)] [M(r) + 4\pi r^3 \rho(r)]}{r[r - 2M(r)]} \quad (1)$$

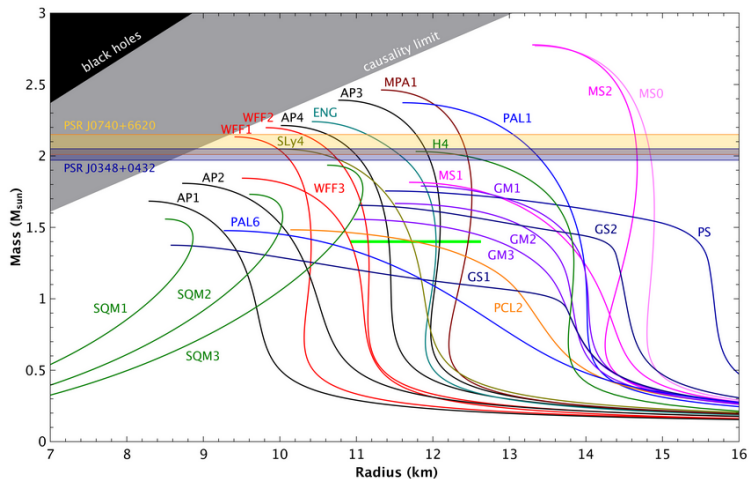
with

$$\frac{dM}{dr} = 4\pi r^2 \varepsilon(r)$$

These are integrated numerically for a specific $\rho(\varepsilon)$

- ▶ For a fixed ε_c central energy density Eq. (1) is **integrated until $\rho = 0$**
- ▶ Varying ε_c a series of compact stars is obtained (with given M and R)
- ▶ Once the maximal mass is reached, the stable series of compact stars ends

MR curves



Observables for dense strongly interacting matter

1. Nuclear physics

▶ $\rho = 0$

nucleon-nucleon scattering, YN and YNN data from femtoscopy (ALICE), BB interaction and potential (lattice: HALQCD)

femtoscopy data and HALQCD calculations are consistent

▶ $\rho \approx \rho_0$

masses of nuclei, isobaric analog states, hypernuclei, giant dipole and pigmy resonances, nuclear dipole polarizabilities, neutron skin thickness \rightarrow normal nuclear density: ρ_0 , binding energy, compressibility, symmetry energy (1st order in asymmetry expanded in density the 0th and 1st term)

2. Perturbative QCD: $\rho \approx 40\rho_0$

N^3 LO calculation, hard thermal loops: $\mu = 2.6$ GeV, $p = 3.8$ GeV/ fm^3 .

T. Gorda, A. Kurkela, et al., Phys. Rev. Lett. 127 (2021) 162003, arXiv:2103.05658.

3. Heavy ion collisions: $\rho : 1 - 8\rho_0$

not very conclusive; there are many competing effects, like momentum dependent interaction, nonequilibrium, nonzero temperature

4. Neutron stars: $\rho : 1 - 8\rho_0$

M, R, Λ . Quite strong constraints even with not yet very precise data

Modelling the strongly interacting matter: Quark-meson model

Plan is to have an interaction with the right global symmetry pattern describing the hadronic (with binding) and the quark phase as well.

1. Starting point is an $SU(3)$ linear sigma model with (pseudo)scalar and (axial)vector nonets. We obtained a very good description for the meson masses and decay widths.

D. Parganlija, P. Kovács, Gy. Wolf, F. Giacosa, D.H. Rischke, Phys. Rev. D87 (2013) 014011

2. We added te isospin breaking

P. Kovács, Gy. Wolf, N. Weickgenannt and D.H. Rischke, Phys. Rev. D (2024)

3. We added the baryon octet and decuplet, baryon masses are from spontaneous breaking of chiral symmetry

P. Kovács, Á. Lukács, J. Váróczy, Gy. Wolf, M. Zétényi, Phys. Rev. D89 (2014) 054004

4. Nonzero temperature, chemical potential: We added Polyakov-loops, quarks: Quark-meson model, very good agreement with lattice at $\mu = 0$.

P. Kovács, Zs. Szép and Gy. Wolf, Phys. Rev. D93 (2016) 114014

Meson fields - pseudoscalar and scalar meson nonets

$$\Phi_{PS} = \sum_{i=0}^8 \pi_i T_i = \frac{1}{\sqrt{2}} \begin{pmatrix} \frac{\eta_N + \pi^0}{\sqrt{2}} & \pi^+ & K^+ \\ \pi^- & \frac{\eta_N - \pi^0}{\sqrt{2}} & K^0 \\ K^- & K^0 & \eta_S \end{pmatrix} (\sim \bar{q}_i \gamma_5 q_j)$$

$$\Phi_S = \sum_{i=0}^8 \sigma_i T_i = \frac{1}{\sqrt{2}} \begin{pmatrix} \frac{\sigma_N + a_0^0}{\sqrt{2}} & a_0^+ & K_S^+ \\ a_0^- & \frac{\sigma_N - a_0^0}{\sqrt{2}} & K_S^0 \\ K_S^- & K_S^0 & \sigma_S \end{pmatrix} (\sim \bar{q}_i q_j)$$

Particle content:

Pseudoscalars: $\pi(138)$, $K(495)$, $\eta(548)$, $\eta'(958)$

Scalars: $a_0(980 \text{ or } 1450)$, $K_0^*(800 \text{ or } 1430)$,

(σ_N, σ_S) : 2 of $f_0(500, 980, 1370, 1500, 1710)$

Included fields - vector meson nonets

$$V^\mu = \sum_{i=0}^8 \rho_i^\mu T_i = \frac{1}{\sqrt{2}} \begin{pmatrix} \frac{\omega_N + \rho^0}{\sqrt{2}} & \rho^+ & K^{*+} \\ \rho^- & \frac{\omega_N - \rho^0}{\sqrt{2}} & K^{*0} \\ K^{*-} & K^{*0} & \omega_S \end{pmatrix}^\mu$$

$$A^\mu = \sum_{i=0}^8 b_i^\mu T_i = \frac{1}{\sqrt{2}} \begin{pmatrix} \frac{f_{1N} + a_1^0}{\sqrt{2}} & a_1^+ & K_1^+ \\ a_1^- & \frac{f_{1N} - a_1^0}{\sqrt{2}} & K_1^0 \\ K_1^- & K_1^0 & f_{1S} \end{pmatrix}^\mu$$

Particle content:

Vector mesons: $\rho(770)$, $K^*(894)$, $\omega_N = \omega(782)$, $\omega_S = \phi(1020)$

Axial vectors: $a_1(1230)$, $K_1(1270)$, $f_{1N}(1280)$, $f_{1S}(1426)$

Lagrangian (2/1)

$$\begin{aligned}
\mathcal{L}_{\text{Tot}} = & \text{Tr}[(D_\mu \Phi)^\dagger (D_\mu \Phi)] - m_0^2 \text{Tr}(\Phi^\dagger \Phi) - \lambda_1 [\text{Tr}(\Phi^\dagger \Phi)]^2 - \lambda_2 \text{Tr}(\Phi^\dagger \Phi)^2 \\
& - \frac{1}{4} \text{Tr}(L_{\mu\nu}^2 + R_{\mu\nu}^2) + \text{Tr} \left[\left(\frac{m_1^2}{2} + \Delta \right) (L_\mu^2 + R_\mu^2) \right] + \text{Tr}[H(\Phi + \Phi^\dagger)] \\
& + c_1 (\det \Phi + \det \Phi^\dagger) + i \frac{g_2}{2} (\text{Tr}\{L_{\mu\nu}[L^\mu, L^\nu]\} + \text{Tr}\{R_{\mu\nu}[R^\mu, R^\nu]\}) \\
& + \frac{h_1}{2} \text{Tr}(\Phi^\dagger \Phi) \text{Tr}(L_\mu^2 + R_\mu^2) + h_2 \text{Tr}[(L_\mu \Phi)^2 + (\Phi R_\mu)^2] + 2h_3 \text{Tr}(L_\mu \Phi R^\mu \Phi^\dagger). \\
& + \bar{\Psi} i \not{\partial} \Psi - g_F \bar{\Psi} (\Phi_S + i\gamma_5 \Phi_{PS}) \Psi + g_V \bar{\Psi} \gamma^\mu \left(V_\mu + \frac{g_A}{g_V} \gamma_5 A_\mu \right) \Psi
\end{aligned}$$

+Polyakov loops

D. Parganlija, P. Kovacs, Gy. Wolf, F. Giacosa, D.H. Rischke, Phys. Rev. D87 (2013) 014011

Lagrangian (2/2)

where

$$D^\mu \Phi = \partial^\mu \Phi - ig_1(L^\mu \Phi - \Phi R^\mu) - ieA_e^\mu [T_3, \Phi]$$

$$\Phi = \sum_{i=0}^8 (\sigma_i + i\pi_i) T_i, \quad H = \sum_{i=0}^8 h_i T_i \quad T_i : U(3) \text{ generators}$$

$$R^\mu = \sum_{i=0}^8 (\rho_i^\mu - b_i^\mu) T_i, \quad L^\mu = \sum_{i=0}^8 (\rho_i^\mu + b_i^\mu) T_i$$

$$L^{\mu\nu} = \partial^\mu L^\nu - ieA_e^\mu [T_3, L^\nu] - \{\partial^\nu L^\mu - ieA_e^\nu [T_3, L^\mu]\}$$

$$R^{\mu\nu} = \partial^\mu R^\nu - ieA_e^\mu [T_3, R^\nu] - \{\partial^\nu R^\mu - ieA_e^\nu [T_3, R^\mu]\}$$

$$\bar{\Psi} = (\bar{u}, \bar{d}, \bar{s})$$

non strange – strange base:

$$\varphi_N = \sqrt{2/3}\varphi_0 + \sqrt{1/3}\varphi_8,$$

$$\varphi_S = \sqrt{1/3}\varphi_0 - \sqrt{2/3}\varphi_8, \quad \varphi \in (\sigma_i, \pi_i, \rho_i^\mu, b_i^\mu, h_i)$$

broken symmetry: non-zero condensates $\langle \sigma_N \rangle, \langle \sigma_S \rangle \longleftrightarrow \phi_N, \phi_S$

Determination of the parameters of the Lagrangian

16 unknown parameters ($m_0, \lambda_1, \lambda_2, c_1, m_1, g_1, g_2, h_1, h_2, h_3, \delta_S, \Phi_N, \Phi_S, g_F, g_V, g_A$) \rightarrow Determined by the **min. of χ^2** :

$$\chi^2(x_1, \dots, x_N) = \sum_{i=1}^M \left[\frac{Q_i(x_1, \dots, x_N) - Q_i^{\text{exp}}}{\delta Q_i} \right]^2,$$

where $(x_1, \dots, x_N) = (m_0, \lambda_1, \lambda_2, \dots)$, $Q_i(x_1, \dots, x_N)$ calculated from the model, while Q_i^{exp} taken from the PDG

multiparametric minimalization \rightarrow **MINUIT**

- ▶ PCAC \rightarrow 2 physical quantities: f_π, f_K
- ▶ Tree-level masses \rightarrow 15 physical quantities:
 $m_{u/d}, m_s, m_\pi, m_\eta, m_{\eta'}, m_K, m_\rho, m_\phi, m_{K^*}, m_{a_1}, m_{f_1^H}, m_{a_0}, m_{K_s}, m_{f_0^L}, m_{f_0^H}$
- ▶ Decay widths \rightarrow 12 physical quantities:
 $\Gamma_{\rho \rightarrow \pi\pi}, \Gamma_{\phi \rightarrow KK}, \Gamma_{K^* \rightarrow K\pi}, \Gamma_{a_1 \rightarrow \pi\gamma}, \Gamma_{a_1 \rightarrow \rho\pi}, \Gamma_{f_1 \rightarrow KK^*}, \Gamma_{a_0}, \Gamma_{K_S \rightarrow K\pi},$
 $\Gamma_{f_0^L \rightarrow \pi\pi}, \Gamma_{f_0^L \rightarrow KK}, \Gamma_{f_0^H \rightarrow \pi\pi}, \Gamma_{f_0^H \rightarrow KK}$
- ▶ $T_c = 155$ MeV from lattice

Inclusion of the vector meson- quark interaction

$$\begin{aligned}\mathcal{L}_{Vq} &= -g_V \sqrt{6} \bar{\Psi} \gamma_\mu V_0^\mu \Psi \\ V_0^\mu &= \frac{1}{\sqrt{6}} \text{diag}(v_0 + \frac{v_8}{\sqrt{2}}, v_0 + \frac{v_8}{\sqrt{2}}, v_0 - \sqrt{2}v_8)\end{aligned}\quad (2)$$

vector fields: like Walecka model, nonzero expectation values are built up at nonzero chemical potential. For simplicity

$$\langle v_0^\mu \rangle = v_0 \delta^{0\mu}, \quad \langle v_8^\mu \rangle = 0$$

Modification of the grand canonical potential:

$$\Omega(T = 0, \mu_q, g_V) = \Omega(T = 0, \tilde{\mu}_q, g_V = 0) - \frac{1}{2} m_V^2 v_0^2,$$

with $\tilde{\mu}_Q = \mu_q - g_V v_0$

Features of our approach

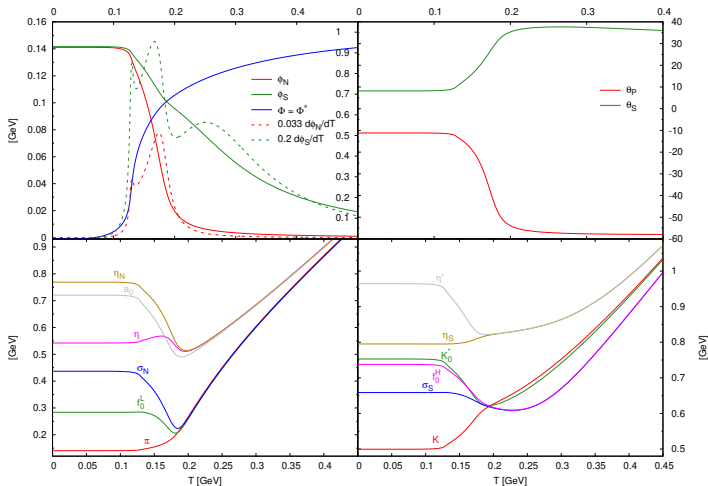
Effective field theory: the same symmetry pattern as in QCD

- ▶ D.O.F's: scalar, pseudoscalar, vector, axial vector nonets,
- ▶ Polyakov loop variables, $\Phi, \bar{\Phi}$ with U^{glue}
- ▶ u,d,s constituent quarks, ($m_u = m_d$)
- ▶ mesonic fluctuations included in the grand canonical potential:

$$\Omega(T, \mu_q) = -\frac{1}{\beta V} \ln(Z)$$

- ▶ Fermion **vacuum** and **thermal** fluctuations
- ▶ Five order parameters ($\phi_N, \phi_S, \Phi, \bar{\Phi}, v_0$) \rightarrow five T/μ -dependent equations

With low mass scalars, $m_{f_0^L} = 300$ MeV

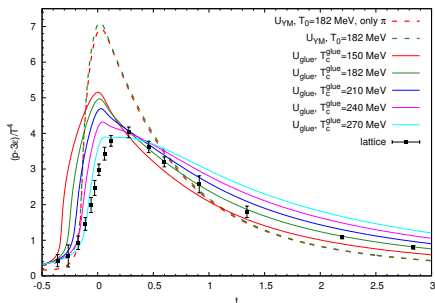


chiral symmetry is restored at high T as the chiral partners (π, f_0^L) , (η, a_0) and (K, K_0^*) , (η', f_0^H) become degenerate

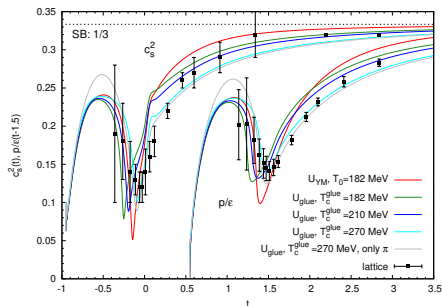
$U(1)_A$ symmetry is not restored, as the axial partners (π, a_0) and (η, f_0^L) do not become degenerate

Observables

interaction measure

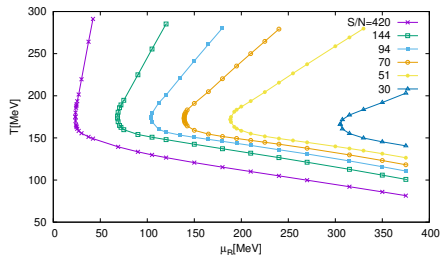


speed of sound



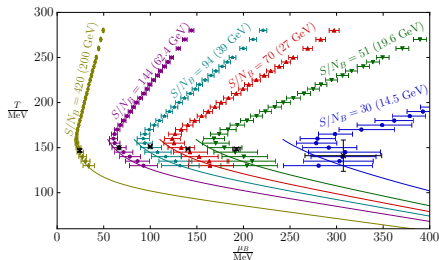
Isentropic trajectories in the $T - \mu_B$ plane

our model, where $\mu_B^{\text{CEP}} > 850 \text{ MeV}$



lattice (analytic continuation)

Günther *et al.*, arXiv:1607.02493



same qualitative behavior of the isentropic trajectories for $\mu_B \leq 400 \text{ MeV}$
 \implies indication that in the lattice result there is no CEP in this region of μ_B

Hadronic EOSs

$$E = E_{vol} + E_{Coulomb} + E_{pairing} + E_{surface} \quad x = \frac{n-n_0}{3n_0}, y = \frac{n_n-n_p}{n}$$

$$E_{vol}(x, y) = E(x, y=0) + E_{symm}(x)y^2 + S_3(x)y^3 + \dots$$

$$E(x, 0) = BE + Kx^2 + Qx^3 + \dots \quad K : \text{incompressibility} = 230 \pm 20 \text{ MeV}$$

Symmetry energy:

$$E_{symm}(x) = J + Lx + K_{symm}/2x^2 + Q_{symm}/6x^3 + \dots$$

$$J = 32 \pm 1 \text{ MeV}; L = 40 - 80 \text{ MeV}, K_{sym} = -200 - +100 \text{ MeV}$$

Affects: NS crust thickness, MR curve

Experimental attemps: nuclear masses, isobaric analog states, neutron skin thicknesses $r_{np} = \sqrt{\langle r_n^2 \rangle} - \sqrt{\langle r_p^2 \rangle}$, nuclear dipole polarizabilities, giant and pygmy dipole resonance energies, flows in heavy-ion collisions
(However PREX neutron skin experiments support higher L (> 100 MeV))

Strangeness: hyperon puzzle ???

EOS

1. $\rho \leq 2 - 4\rho_0$ ordinary nuclear potentials, CEFT, ...
2. $2 - 4\rho_0 \leq \rho \leq 6 - 8\rho_0$ quark matter model
3. $6 - 8\rho_0 \leq \rho$ extrapolation to the pQCD point

hadronic matter - soft: SFHo

(Steiner, A. W., Hempel, M., Fischer, T. *Astrophys. J.* 774 (2013) 17) and Hempel, M., Schaffner-Bielich, J. *Nucl. Phys.* A837 (2010) 210)

relativistic mean-field model (nucleons, σ, ω, ρ with quartic couplings), with $K=245$ MeV, $L=47.1$ MeV, $m^*/m_n=0.76$.

hadronic matter - stiff: DD2

(S. Typel, et al., *Phys. Rev.* C81 (2010) 015803)

relativistic mean-field + light clusters, $K = 243$ MeV, $L=58$ MeV $m^*/m_n=0.63$

Quark matter: Quark-meson model - chiral $U(3) \times U(3) \rightarrow SU(2) \times U(1)$ model
 degrees of freedom: 4 meson nonets, constituent quarks, Polyakov loops
 condensates: 2 scalar (N,S), Polyakov loops ($T > 0$), vector mesons ($\mu > 0$)

P. Kovács, Zs. Szép, Gy. Wolf, *Phys. Rev.* D93 (2016) 114014

Concatenation

It seems that a strong first order phase transition is ruled out by astrophysical constraints: J.-E. Christian and J. Schaffner-Bielich, Phys. Rev. D 103, 063042 (2021),
The allowed $p(\varepsilon)$ functions are in a rather narrow band, there can be no big jump

Hadron-quark crossover with polynomial interpolation ($\rho = \rho_B$):

$$\varepsilon(\rho_B) = \varepsilon_{hadronic}(\rho_B) \quad \rho_B < \rho_{BL},$$

$$\varepsilon(\rho_B) = \sum_{k=0}^5 C_k \rho_B^k \quad \rho_{BL} \leq \rho_B \leq \rho_{BU}$$

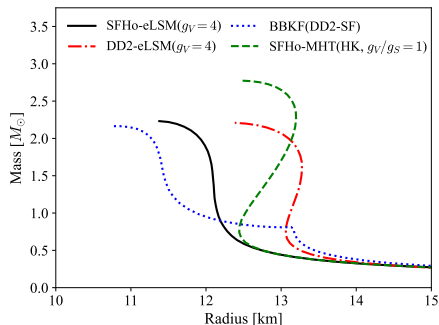
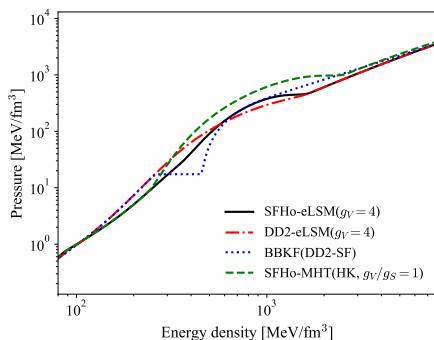
$$\varepsilon(\rho_B) = \varepsilon_{qm}(\rho_B) \quad \rho_{BU} < \rho_B.$$

C_k is determined by the requirement that the energy density, ε and its first two derivatives with respect to ρ_B , pressure and sound velocity is continuous at the boundaries.

2 parameters: $\Gamma = 0.5 * (\rho_{BU} - \rho_{BL})$ and $\overline{\rho_B} = 0.5 * (\rho_{BL} + \rho_{BU})$

EOSs used in our studies

- ▶ SFHo + eLSM
- ▶ DD2 + eLSM
- ▶ SFHo + Masuda-Hatsuda quark model
- ▶ BBKF including first order phase transition

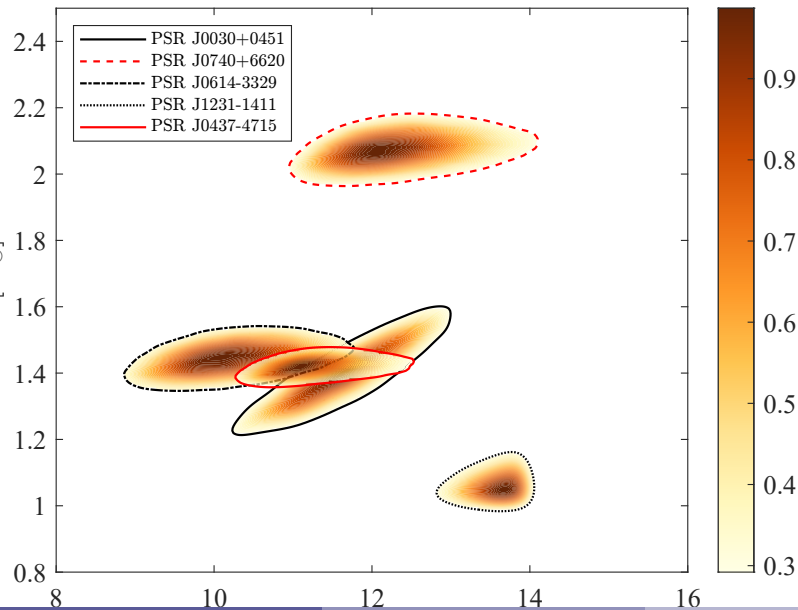


Left panel: Equations of state considered in this work, including polynomially matched hadron–quark constructions based on the SFHo and DD2 hadronic EoSs, as well as an equation of state featuring a first-order phase transition. 26

Data

- ▶ **perturbative QCD** EOS should converge to it keeping $c_s < 1$,
 $\mu_{QCD} = 2.6 \text{ GeV}$, $n_{QCD} = 6.471 / \text{fm}^3$, $\rho_{QCD} = 3823 \text{ MeV} / \text{fm}^3$
- ▶ **Minimal TOV mass constraint**: $M_{TOV}^{min} = 2.22 M_\odot$: PSR J0952–0607 a black widow pulsar, with a mass $2.35 \pm 0.17 M_\odot$,
 There are several pulsars mass above $2M_\odot$, using population analysis at the 1σ confidence level $M_{TOV}^{min} = 2.22 M_\odot$
- ▶ **NICER**: (M,R) values for PSR J0030+0451, PSR J0740+6620, PSR J0614–3329, PSR J1231–1411, and PSR J0437–4715
- ▶ **tidal deformability** GW170817: : $70 < \Lambda(1.4 M_\odot) < 720$ Abbot (2019)
 stronger constraint: $70 < \Lambda_{1.4} < 580$, $9.1 \text{ km} < R_{1.4} < 12.8 \text{ km}$
- ▶ **Hess J1731-347** neutron star: mass= $0.77 \pm 0.19 M_\odot$, $R = 10.4 \pm 0.8 \text{ km}$
- ▶ **massgap neutron star**: $2.59 \pm 0.09 M_\odot$

NICER data



Bayesian inference

Unsetted parameters: $m_\sigma, g_v, \bar{\rho}_B \equiv 0.5(\rho_{BL} + \rho_{BU}), \Gamma \equiv 0.5(\rho_{BU} - \rho_{BL})$

$$290 \text{ MeV} \leq m_\sigma \leq 700 \text{ MeV}$$

$$0 \leq g_v \leq 10$$

$$2\rho_0 \leq \bar{\rho}_B \leq 5\rho_0$$

$$\rho_0 \leq \Gamma \leq 4\rho_0 \quad \text{with the constraint: } \rho_{BL} = \bar{\rho}_B - \Gamma > \rho_0$$

We created ~ 18000 EOSs to be used in the Bayesian analysis

Bayes theorem:

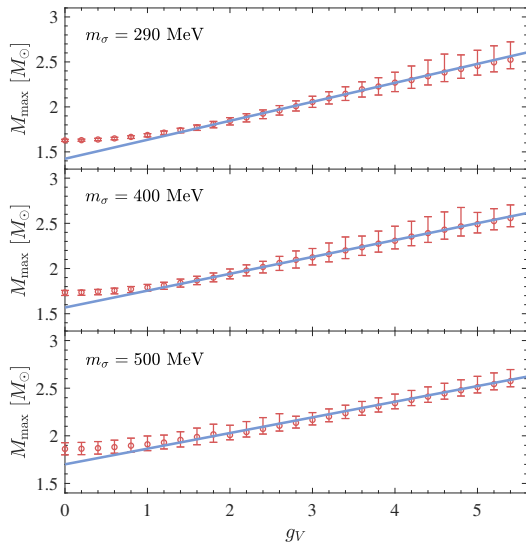
θ is a parameter set, $p(\theta)$ is the prior probability for θ , $p(\text{data}|\theta)$ is the probability that for given θ , the data is measured. Then

$$p(\theta|\text{data}) = \frac{p(\text{data}|\theta)p(\theta)}{p(\text{data})}$$

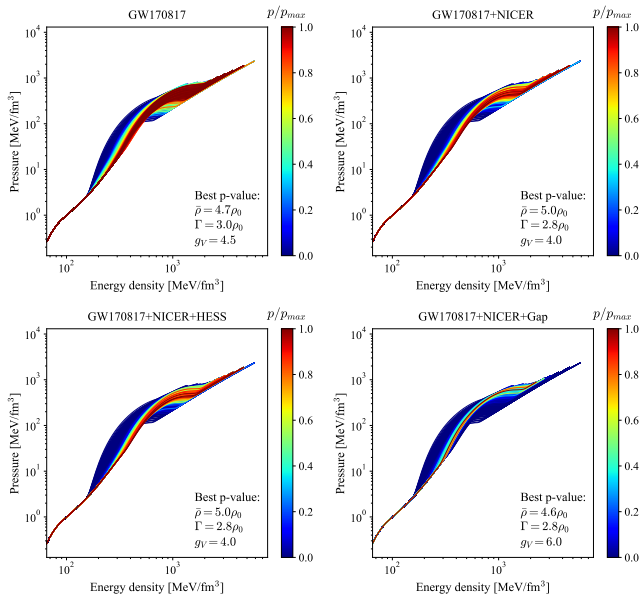
$p(\text{data})$ is a normalization constant. We assume $p(\theta)$ is uniform in the allowed hypersurface. For independent observations:

$$p(\text{data}|\theta) = p(M_{\text{max}}|\theta)p(\text{NICER}|\theta)p(\bar{\Lambda}|\theta)$$

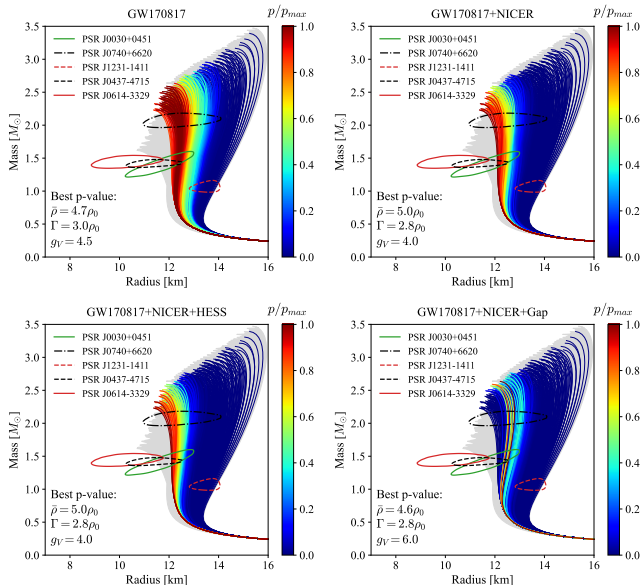
Phys. Rev. D105 (2022) 103014, Phys. Rev. D108 (2023) 043002.

g_V dependence of the M_{max} 

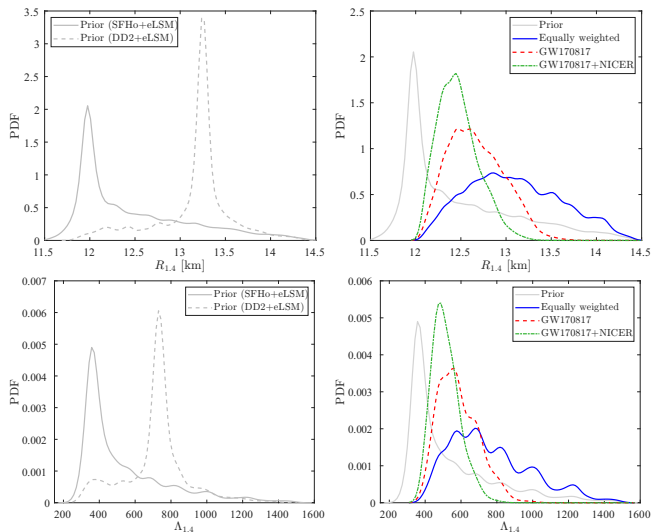
The errorbars are obtained by varying $\bar{\rho}$ and Γ .



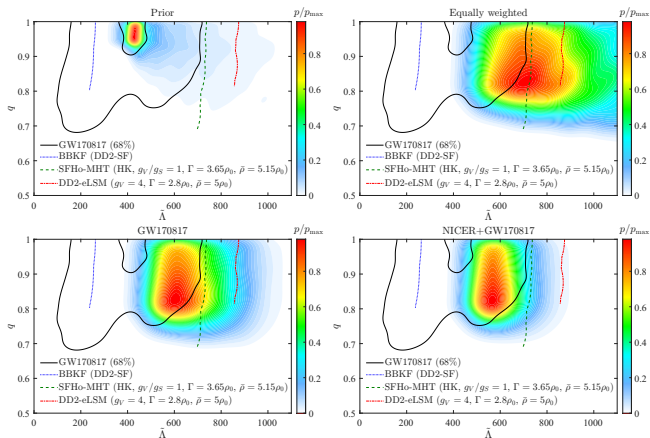
M(R) probabilities



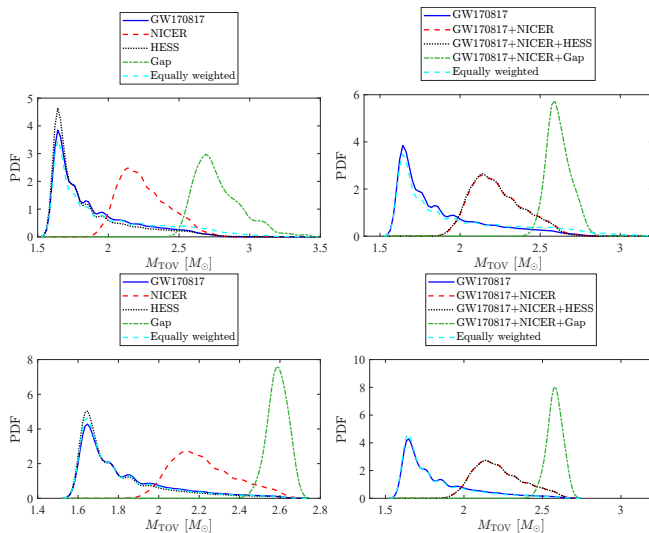
PDF of the radii and tidal deformabilities



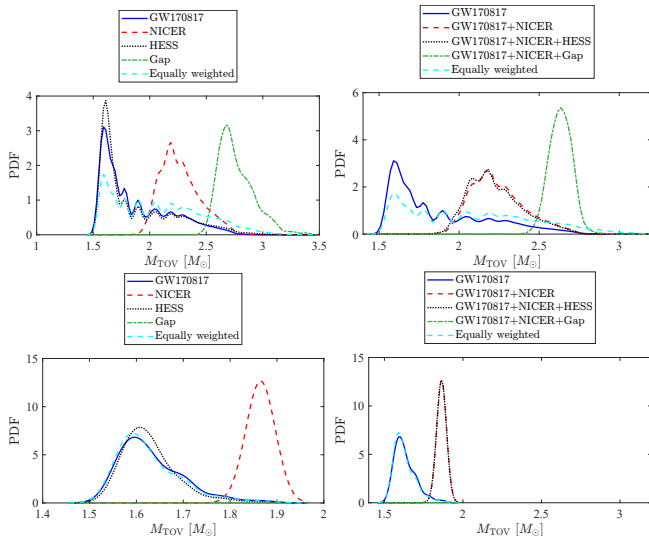
2D of compactness and tidal deformabilities



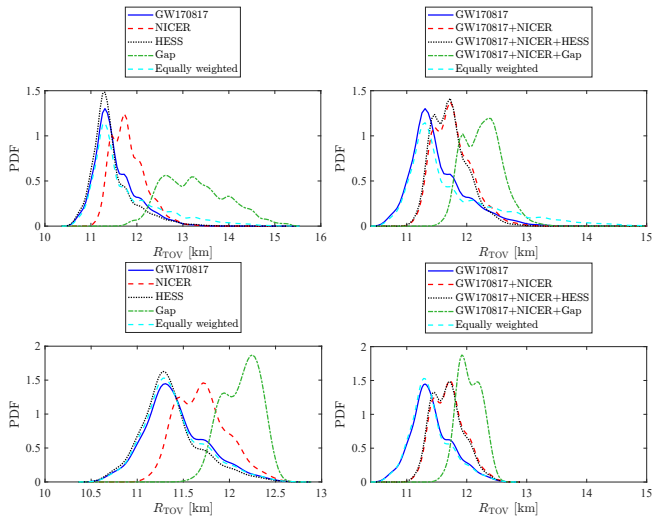
Distribution of the maximal mass (SFHo and DD2)

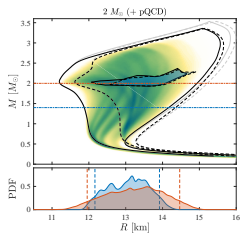


Maximal mass (SFHo and DD2) with strong GW constraint

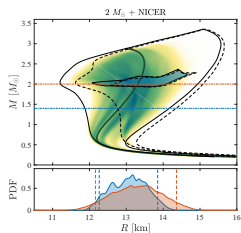


Distribution of the R_{TOV} (SFHo and DD2)

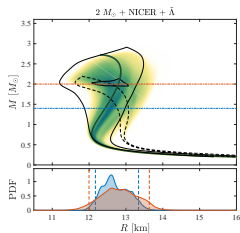


Distribution of $M(R)$ curves

prior ($M_{max} + pQCD$)

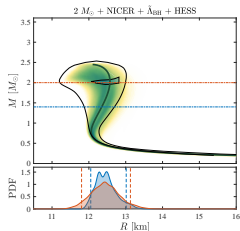


prior + NICER

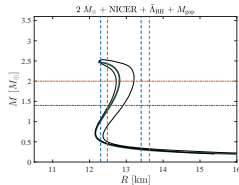


prior + NICER + GW

Distribution of $M(R)$ curves

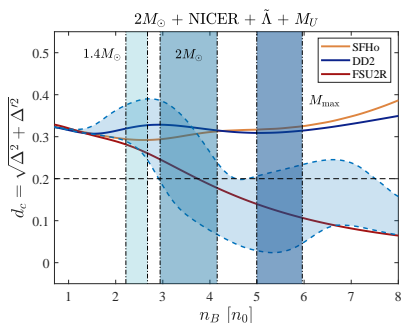
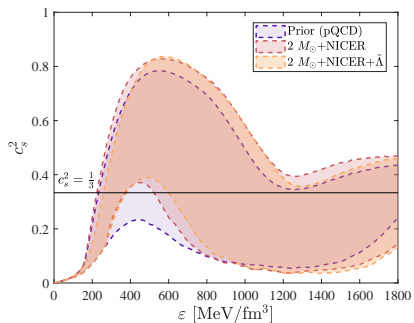


prior + NICER + GW
+ HESS

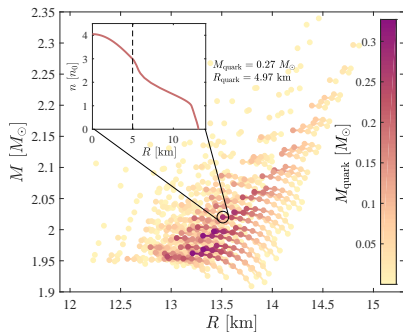
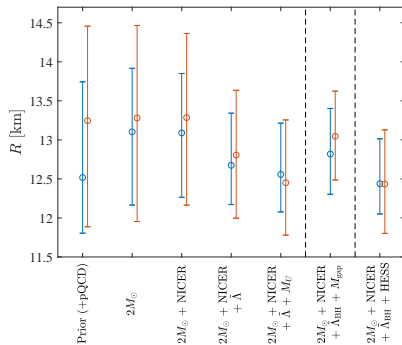


prior + NICER + GW
+ Mgap

Sound velocity



Radius and Quark content



Summary and Conclusions

- ▶ Our model can reproduce the lattice calculations at $\mu = 0$
- ▶ With our model we can fulfill the present astronomical constraints
- ▶ The central density do not go above $6\rho_0$.
- ▶ The radius of the neutron stars are 12.8 ± 0.8 km.
- ▶ strangeness should be included into the hadronic model
- ▶ hadronic and quark phase ought to be handled with the same model to drop ad-hoc parameters

Thank you for your attention!

Polyakov loops in Polyakov gauge

Polyakov loop variables: $\Phi(\vec{x}) = \frac{\text{Tr}_c L(\vec{x})}{N_c}$ and $\bar{\Phi}(\vec{x}) = \frac{\text{Tr}_c \bar{L}(\vec{x})}{N_c}$ with

$$L(x) = \mathcal{P} \exp \left[i \int_0^\beta d\tau A_4(\vec{x}, \tau) \right]$$

→ signals center symmetry (\mathbb{Z}_3) breaking at the deconfinement

low T : confined phase, $\langle \Phi(\vec{x}) \rangle, \langle \bar{\Phi}(\vec{x}) \rangle = 0$

high T : deconfined phase, $\langle \Phi(\vec{x}) \rangle, \langle \bar{\Phi}(\vec{x}) \rangle \neq 0$

Polyakov gauge: the temporal component of the gauge field is time independent and can be gauge rotated to a diagonal form in the color space

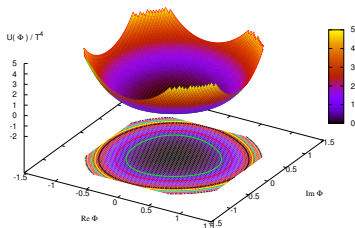
Effects of the gauge fields:

- ▶ In this gauge the effect of the gauge field on the quarks acts like an imaginary chemical potential
→ modified quark distribution function.
- ▶ **Polyakov potential:** $\mathcal{U}(\Phi, \bar{\Phi})$ models the free energy of a pure gauge theory, parameters are fitted to the pure gauge lattice data

Polyakov loop potential

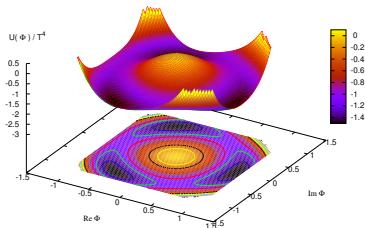
“Color confinement”

$\langle \Phi \rangle = 0 \rightarrow$ no breaking of \mathbb{Z}_3
one minimum



“Color deconfinement”

$\langle \Phi \rangle \neq 0 \rightarrow$ spontaneous breaking of \mathbb{Z}_3
minima at $0, 2\pi/3, -2\pi/3$
one of them spontaneously selected



from H. Hansen et al., PRD75, 065004 (2007)

Effects of Polyakov loops on FD statistics

Inclusion of the Polyakov loop modifies the Fermi-Dirac distribution function

$$f(E_p - \mu_q) \rightarrow f_{\Phi}^+(E_p) = \frac{(\bar{\Phi} + 2\Phi e^{-\beta(E_p - \mu_q)}) e^{-\beta(E_p - \mu_q)} + e^{-3\beta(E_p - \mu_q)}}{1 + 3(\bar{\Phi} + \Phi e^{-\beta(E_p - \mu_q)}) e^{-\beta(E_p - \mu_q)} + e^{-3\beta(E_p - \mu_q)}}$$

$$f(E_p + \mu_q) \rightarrow f_{\Phi}^-(E_p) = \frac{(\Phi + 2\bar{\Phi} e^{-\beta(E_p + \mu_q)}) e^{-\beta(E_p + \mu_q)} + e^{-3\beta(E_p + \mu_q)}}{1 + 3(\Phi + \bar{\Phi} e^{-\beta(E_p + \mu_q)}) e^{-\beta(E_p + \mu_q)} + e^{-3\beta(E_p + \mu_q)}}$$

$$\Phi, \bar{\Phi} \rightarrow 0 \implies f_{\Phi}^{\pm}(E_p) \rightarrow f(3(E_p \pm \mu_q))$$

$$\Phi, \bar{\Phi} \rightarrow 1 \implies f_{\Phi}^{\pm}(E_p) \rightarrow f(E_p \pm \mu_q)$$

three-particle state appears: mimics confinement of quarks within baryons

at $T = 0$ there is no difference between models with and without Polyakov loop